A MODULAR OPTIMIZATION FRAMEWORK FOR 4TH GENERATION LIGHT SOURCE LATTICE DESIGN: SYNERGIZING PHYSICS PRIORS AND STATISTICAL LEARNING

L. L. Mao*, Shanghai Institute of Applied Physics, CAS, Shanghai, China
S. Q. Tian, X. Z. Liu, L. Y. Tan, Shanghai Advanced Research Institute, CAS, Shanghai, China
Y. H. Gong, Shanghai Synchrotron Radiation Facility, Shanghai, China

Abstract

The design of fourth-generation synchrotron light sources based on Hybrid Multi-Bend Achromat (H-MBA) structures faces significant challenges due to the high dimensionality of design variables and the strong nonlinear effects induced by strong focusing forces. The traditional paradigm of "manual matching followed by stepwise fine-tuning" encounters bottlenecks in optimization efficiency and physical interpretability. This paper proposes a modular optimization framework that fuses physics priors with statistical learning to achieve synergistic optimization of linear optics and nonlinear dynamics. The framework uses Twiss parameter evolution as an intermediate physical representation, and a physics-prior screening mechanism driven by linear transport is combined with the Covariance Matrix Adaptation Evolution Strategy (CMA-ES). This approach identifies stable periodic solutions with reduced natural emittance within minutes and shows reproducible efficiency gains over manual initializations. Machine-learning classifiers trained on the generated dataset perform high-confidence pruning of the solution space and retain high-quality solutions. A local trust region constructed around these "promising solutions" introduces the Sequential Model-based Algorithm Configuration (SMAC) strategy based on Random Forests for refined iteration. This method provides an efficient and intelligent pathway for complex, high-dimensional lattice design.

INTRODUCTION

Fourth-generation synchrotron light sources based on hybrid multi-bend achromat (H-MBA) lattices require joint control of low natural emittance, periodic linear optics, chromatic correction, dynamic aperture (DA), and energy acceptance (EA) [1]. The lattice considered in this paper is a 3.5 GeV ring with a circumference of 406.6 m. Strong focusing and compact dispersion bumps in an H7BA cell produce a constrained search space. Nonlinear tracking can reject a candidate with excellent linear emittance.

The present work treats lattice design as a staged physics-and-data workflow rather than as a single black-box minimization. Twiss parameter evolution through the cell is used as an intermediate physical representation. The optimizer searches for periodic and interpretable linear optics and passes selected candidates to statistical screening, local acquisition, and final DA/EA validation [2].

* maolinglong@sinap.ac.cn

MODULAR OPTIMIZATION METHOD

Physics-prior CMA-ES

The physics-prior module uses linear transport and Twiss evolution to reject candidates that do not return to the desired cell boundary. The boundary conditions include $\beta_x \simeq 5$ m, $\beta_y \simeq 3$ m, $\alpha_{x,y} \simeq 0$, and dispersion close to zero. These quantities give the search a direct optical meaning prior to expensive nonlinear calculations.

CMA-ES acts on the physics-filtered magnet-strength variables, namely the K-value vector used by the lattice model [3]. Parallel runs on 24 cores identify stable low-emittance periodic optics within minutes. Figure 1 shows the adaptation of the sampled search distribution.

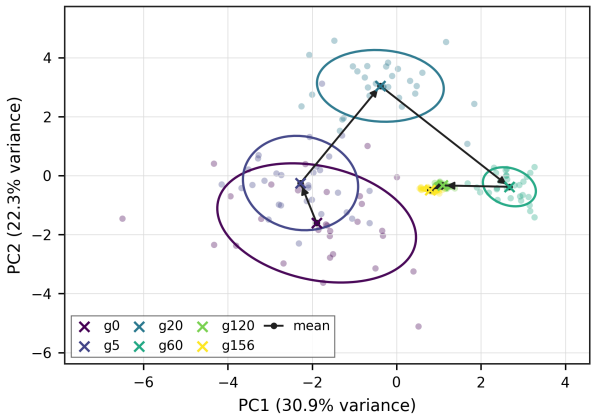

Figure 1: CMA-ES Gaussian search distributions projected onto the first two principal components. The coloured contours show 1.5σ covariance envelopes for selected generations, and the black curve follows the sampled mean path.

RF Pruning and SMAC-style Acquisition

The generated candidate pool is converted into a labelled data set for Random-Forest (RF) screening [4], as summarized in Fig. 2. The aggregated data set contains 11928 unique lattice-candidate rows from 35 computation batches, covering CMA-ES branches, trust-region DA scans, GPU-SMAC trials, and ML trust-region proposals. Labels are assigned from the corresponding optics checks, EA scans, quality criteria, and DA tracking outputs.

Four RF classifiers were trained for physics evaluability, EA acceptance, high-quality retention, and DA-promising identification. Figure 3 summarizes their ROC-AUC values. The physics, EA, and high-quality classifiers provide robust

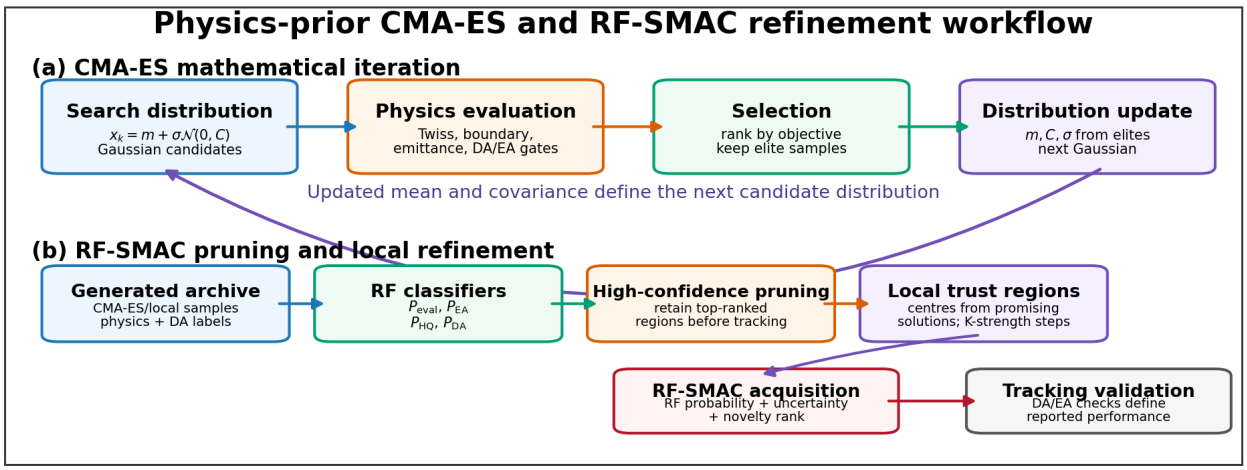

Figure 2: Combined optimization workflow. (a) The CMA-ES mathematical iteration, where ranked physics-evaluated samples update the mean, covariance, and step size of the next candidate distribution. (b) RF pruning and RF-SMAC local refinement; ML scores accelerate candidate selection, and tracking validation defines the final reported performance.

pruning, with ROC-AUC values of 0.949, 0.973, and 0.981. As shown in Fig. 4, the representative feature-importance distributions illustrate the dominant variables for these classifiers. The rare DA-promising label reaches ROC-AUC 0.980 and serves as a ranking signal prior to tracking.

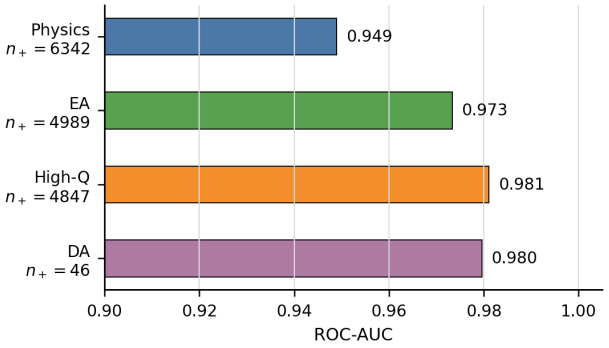

Figure 3: ROC-AUC values of the four Random-Forest classifiers used for candidate-pool pruning and candidate ranking. The positive sample count is shown for each label.

The SMAC-style module constructs trust regions around promising candidates and ranks local samples using RF probability, ensemble uncertainty, and a novelty term [5]. As illustrated in Fig. 5, this ranking strategy ensures that the candidates retain high predicted quality. The RF-SMAC step then generated a 200-candidate local pool for final validation.

RESULTS

Workflow Performance

The proposed workflow generates physics-evaluable candidates first and reserves tracking for selected promising solutions. Final validation is separated from all proxy and classifier scores. EA is reported in the negative and positive momentum directions, denoted as EA− and EA+; DA is evaluated with action-based tracking, where initial amplitudes

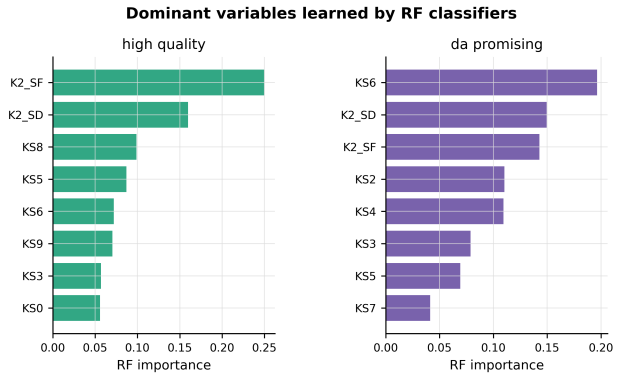

Figure 4: Representative RF feature-importance distributions for the high-quality and DA-promising labels. The ranking shows which magnet-strength variables dominate the classifier decisions used for candidate pruning.

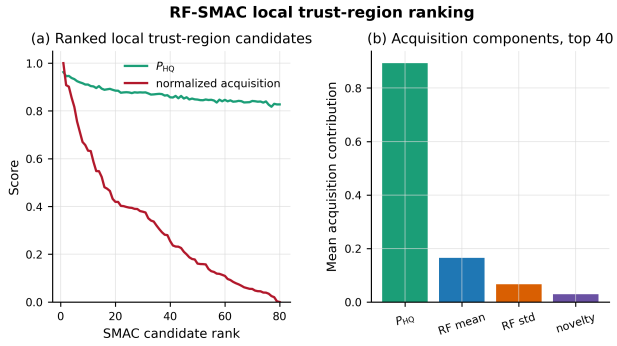

Figure 5: RF-SMAC local trust-region ranking. The ranked candidates retain high predicted quality while the acquisition function combines RF probability, model uncertainty, and novelty.

are generated from Courant-Snyder normalized phase-space action coordinates.

Table 1: Validated Candidates from the Modular Workflow

Candidate	Emit. [pm]	EA− [%]	EA+ [%]	DA− [mm]	DA+ [mm]	DA area [mm^2]
G00-000	115.88	-2.47	2.20	-2.33	1.33	10.11
G04-013	96.97	-2.47	2.07	-2.00	4.17	30.04
G09-023	97.02	-2.47	2.07	-1.83	4.33	29.18
G10-020	97.67	-2.47	2.07	-2.00	4.17	29.87
G14-020	97.60	-2.53	2.13	-1.67	4.50	28.12
G15-005	96.29	-2.40	2.07	-1.83	4.17	26.19
G18-003	96.21	-2.47	2.07	-1.83	4.00	31.20
G26-021	96.30	-2.47	2.07	-1.83	4.50	29.20

Sub-100 pm Solutions

The same modular workflow produced new low-emittance solutions that were verified by 6D multi-particle tracking. The sub-100 pm candidates listed in Table 1 have minimum stable energy deviation above 2% and nonzero transverse tracking acceptance. Table 1 includes G00-000, the validated CMA-ES solution used to initialize the local trust-region search.

The local trust-region search used G00-000 as the initial point, which passed the same tracking definition with 115.88 pm emittance, EA− = −2.47%, EA+ = 2.20%, DA− = −2.33 mm, DA+ = 1.33 mm, and 10.11 mm^2 DA area. The representative solution G10-020 was obtained at generation 10. The search from G00-000 to G10-020 took about 9.9 min; the independent tracking validation took 484 s. The emittance is reduced from 115.88 to 97.67 pm, and the DA area increases from 10.11 to 29.87 mm^2. Figure 6 shows the corresponding evolution.

Local Trust-region Refinement

The local refinement module follows RF pruning and concentrates evaluations around promising candidates. Its role is to improve the efficiency of the final validation stage, not to replace tracking. Figure 6 shows that selected validated candidates move from the initial tracked point to a cluster of sub-100 pm candidates with larger DA area.

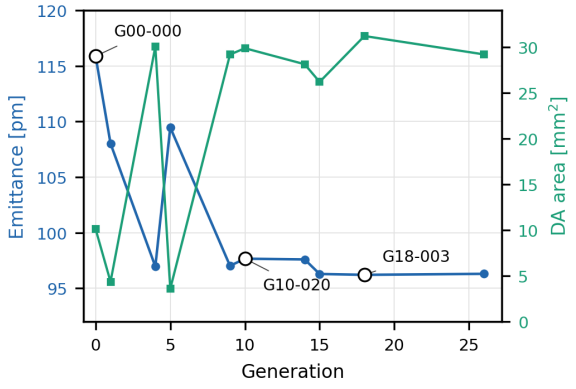

Figure 6: Trust-region evolution from the physics-prior seed. The blue curve shows the natural emittance of selected validated candidates, and the green curve shows the corresponding symmetric DA area.

CONCLUSION

A modular H7BA optimization framework combining Twiss-evolution physics priors, CMA-ES, RF pruning, RF-SMAC local acquisition, and final DA/EA validation has been demonstrated. Through this workflow, seven sub-100 pm candidates were verified by 6D multi-particle tracking with natural emittance of 96.21 – 97.67 pm, EA− of −2.53 – −2.40%, EA+ of 2.07 – 2.13%, DA− of −2.00 – −1.67 mm, DA+ of 4.00 – 4.50 mm, and symmetric DA area of 26.19 – 31.20 mm^2. Starting from the validated CMA-ES solution G00-000, the final candidate G10-020 is reached within 10 trust-region generations, reducing emittance by 15.7% and increasing the DA area by a factor of 2.95. These results demonstrate that physics-prior search and statistical learning can be combined into a traceable workflow for high-dimensional lattice optimization when final claims are tied to stated tracking definitions.

REFERENCES

[1] J. Tan, J. Xu, P. Yang, Z. Bai, and L. Wang, "Hybrid multibend achromat lattice with sextupole cancellation across a straight section," *Phys. Rev. Accel. Beams*, vol. 26, no. 12, p. 121602, 2023. doi:10.1103/PhysRevAccelBeams.26.121602

[2] Y. Lu *et al.*, "Demonstration of machine learning-enhanced multi-objective optimization of ultrahigh-brightness lattices for 4th-generation synchrotron light sources," *Nucl. Instrum. Methods Phys. Res. A*, vol. 1050, p. 168192, 2023. doi:10.1016/j.nima.2023.168192

[3] N. Hansen, "The CMA evolution strategy: a comparing review," in *Towards a new evolutionary computation: advances in estimation of distribution algorithms*, J. A. Lozano, P. Larranaga, I. Inza, and E. Bengoetxea, Eds. Berlin, Heidelberg, Germany: Springer, 2006, pp. 75–102. doi:10.1007/11007937_4

[4] L. Breiman, "Random forests," *Mach. Learn.*, vol. 45, no. 1, pp. 5–32, 2001. doi:10.1023/A:1010933404324

[5] F. Hutter, H. H. Hoos, and K. Leyton-Brown, "Sequential model-based optimization for general algorithm configuration," in *Proc. LION'2011*, Rome, Italy, Jan. 2011, LNCS, vol. 6683, pp. 507–523. doi:10.1007/978-3-642-25566-3_40